

## SUPPLEMENTAL INFORMATION

### **Electrokinetically Driven Fluidic Transport in Integrated Three-Dimensional Microfluidic Devices Incorporating Gold-Coated Nanocapillary Array Membranes**

Aigars Piruska,<sup>1</sup> Sean Branagan,<sup>1</sup> Donald M. Cropek,<sup>2</sup> Jonathan V. Sweedler<sup>3</sup> and Paul  
W. Bohn<sup>1\*</sup>

<sup>1</sup>Department of Chemical and Biomolecular Engineering, University of Notre Dame,  
Notre Dame, IN 46556

<sup>2</sup>U.S. Army Engineering Research and Development Center, P.O. Box 9005, Champaign,  
IL 61826-9005

<sup>3</sup>Department of Chemistry, University of Illinois at Urbana-Champaign, 600 S. Mathews  
Ave., Urbana, IL 61801

### Bubble formation in a microfluidic channel

The model presented here describes current density at an electrically floating electrode as a function of (a) spatial coordinates, (b) potential gradient and (c) a given set of redox couples. The model entails the following assumptions: (a) a linear potential variation along the length of the electrode; (b) Faradaic currents determined in accord with the Butler-Volmer equation<sup>1</sup>, *i.e.* electron transfer is rate limiting; and (c) anodic and cathodic currents are equal in magnitude, *i.e.* no charging of the electrode occurs.

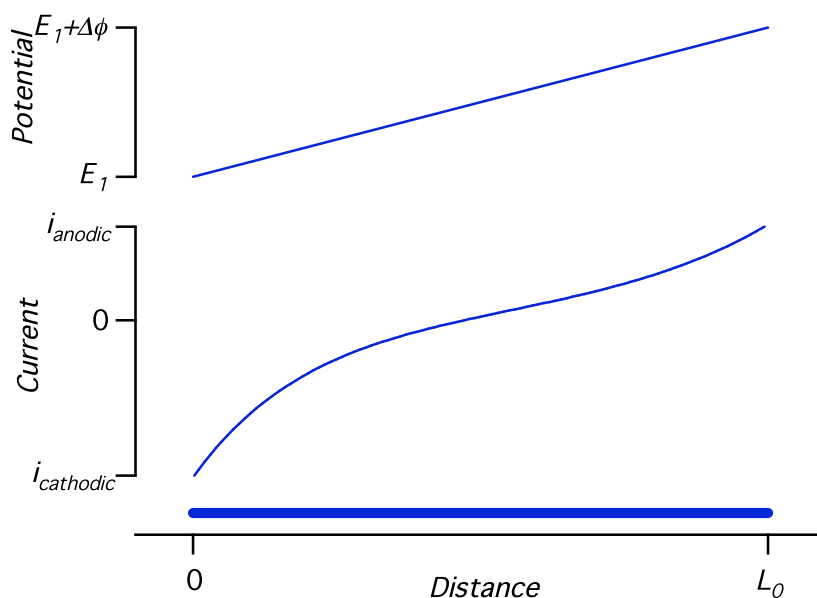


Figure S1. Schematic diagram of model for water electrolysis. The spatial coordinate system, assumed potential distribution, and an example of a typical current distribution are shown.

An electric field with strength  $V$  is applied in parallel with the electrode of length  $L_0$ , and causes potential drop  $\Delta\phi$  across the electrode (see Figure S1):

$$V = \frac{\Delta\phi}{L_0} \quad (1)$$

Current density for both, anodic and cathodic, processes is described by:

$$i = i_{0,l} \left[ \exp\left(\frac{-\alpha_l n_l F (E - E_l^0)}{RT}\right) - \exp\left(\frac{(1 - \alpha_l) n_l F (E - E_l^0)}{RT}\right) \right] \quad (2)$$

Subscript  $l$  indicates anodic or cathodic process,  $\alpha$  is the transfer coefficient,  $n$  the number of electrons,  $i_0$  the exchange current, and  $E^0$  is the standard potential. The current in the Au membrane electrode can be obtained by integrating eqn. (2), yielding:

$$\begin{aligned} I(x_1, x_2) &= \int_{x_1}^{x_2} w i(x) dx = \\ &= \int_{x_1}^{x_2} w i_{0,l} \left[ \exp\left(\frac{-\alpha_l n_l F (E_1 + Vx - E_l^0)}{RT}\right) - \exp\left(\frac{(1 - \alpha_l) n_l F (E_1 + Vx - E_l^0)}{RT}\right) \right] dx = \\ &= \frac{-w i_{0,l} RT}{FV} \left[ \frac{1}{\alpha_l n_l} \exp\left(\frac{-\alpha_l n_l F (E_1 + Vx - E_l^0)}{RT}\right) \right]_{x_1}^{x_2} + \frac{1}{(1 - \alpha_l) n_l} \exp\left(\frac{(1 - \alpha_l) n_l F (E_1 + Vx - E_l^0)}{RT}\right) \right]_{x_1}^{x_2} \end{aligned} \quad (3)$$

where  $E_1$  is electrode potential at the cathode end and  $w$  is the width of the electrode. For an irreversible process, such as solvent electrolysis, anodic (cathodic) current below (above) the standard potential is essentially zero and can be ignored. Thus, cathodic current should be integrated between  $x_l = 0$  and  $x_2 = (E_c^0 - E_l)/V$ , giving:

$$I_c = \frac{-w i_{0,c} RT}{FV} \left[ \frac{1}{\alpha_c n_c} \left( 1 - \exp\left(\frac{-\alpha_c n_c F (E_1 - E_c^0)}{RT}\right) \right) + \frac{1}{(1 - \alpha_c) n_c} \left( 1 - \exp\left(\frac{(1 - \alpha_c) n_c F (E_1 - E_c^0)}{RT}\right) \right) \right] \quad (4)$$

Anodic current should be integrated between  $x_l = (E_a^0 - E_l)/V$  and  $x_2 = L_0$ , giving:

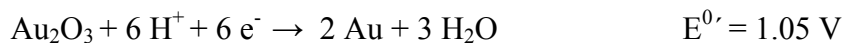
$$I_a = \frac{-wi_{0,a}RT}{FV} \left[ \frac{1}{\alpha_a n_a} \left( \exp \left( \frac{-\alpha_a n_a F (E_1 + L_0 - E_a^0)}{RT} \right) - 1 \right) + \frac{1}{(1-\alpha_a)n_a} \left( \exp \left( \frac{(1-\alpha_a)n_a F (E_1 + L_0 - E_a^0)}{RT} \right) - 1 \right) \right] \quad (5)$$

The value of  $E_1$  can be found by requiring the anodic and cathodic currents to be of equal magnitude,  $I_c = -I_a$ .

The assumption of kinetically limiting electron transfer is reasonable for electrochemical breakdown of water, by far the major electroactive component of the running buffer. Relevant half-reactions and their formal potentials at pH=7 are indicated below.



It must be noted that gold oxidation occurs at very similar potentials to oxygen evolution, but was not considered in the model:



The charge needed to generate a gas bubble that can occlude a channel of dimensions  $[50 \mu\text{m}]^3$ ,  $\sim 10^{-6}$  C, or to form saturated  $\text{H}_2$  or  $\text{O}_2$  solution in running buffer ( $\sim 10^{-8}$  C) can be calculated purely based on stoichiometric considerations. Thus, a potential drop in parallel with the Au-NCAM large enough to lead to  $\sim 10^{-6}$  A current was used as the indication of bubble formation in the model

The kinetics of  $\text{H}_2$  and  $\text{O}_2$  evolution have been studied in considerable detail, using both gold and platinum as model systems, and an extensive review by Conway is available.<sup>2</sup> Oxygen and hydrogen evolution at gold electrodes have mainly been studied in acidic ( $1 \leq \text{pH} \leq 2$ ) or basic ( $12 \leq \text{pH} \leq 14$ ) media; few studies report data on processes at neutral pH. Kinetic data are typically given as Tafel plot parameters (slope,  $b$ , and

exchange current density,  $i_0$ , or intercept in overpotential,  $\eta$ , vs. current density,  $\log i$ ). Kinetic parameters for oxygen evolution at both low and high pH are very similar,<sup>3</sup> so we assume that these parameters are also appropriate near pH 7 and use  $b = 0.045$  V and  $i_0 = 1.6 \times 10^{-22}$  A cm<sup>-2</sup> for the model. Tafel parameters for hydrogen evolution are more pH sensitive and were estimated from Ohmori and Enyo<sup>4</sup> as  $b = 0.120$  V and  $i_0 = 10^{-7}$  A cm<sup>-2</sup>.

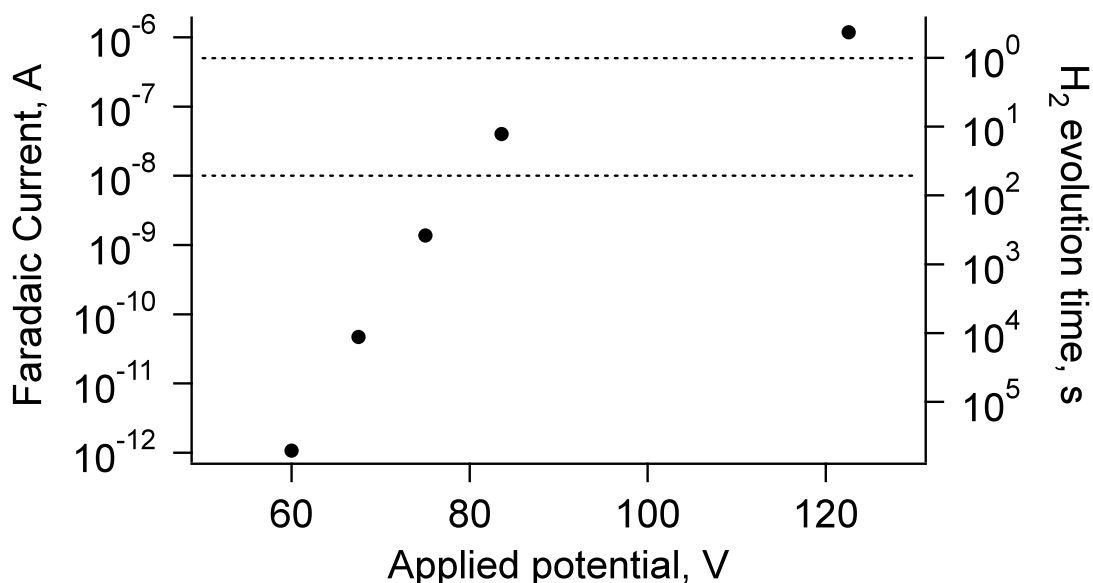


Figure S2. Modeled Faradaic current in gold segment due to applied potential across microfluidic channel. H<sub>2</sub> evolution time calculated from stoichiometric consideration, assuming that [50 μm]<sup>3</sup> of gas are required to block the channel. Top line indicates current, large enough to form gas bubble instantaneously (within 1 s), bottom line – forming saturated gas solution in water.

Applying these parameters and conditions the model predicts that bubble formation occurs when 120 V is applied along a 12 mm long microfluidic channel, resulting in a 3V potential drop along a 400 μm gold segment (see Fig. S2). The resulting spatial current density distribution is shown in Fig. S3. Consistent with the qualitative

reasoning above, the model shows that the vast majority of electrochemical processes occur near (within  $\sim 10 \mu\text{m}$ ) the edges of the bipolar gold electrode. This is also consistent with visual observations. Several caveats must be considered in interpreting these results. First, the calculated current density is large and outside the range of current

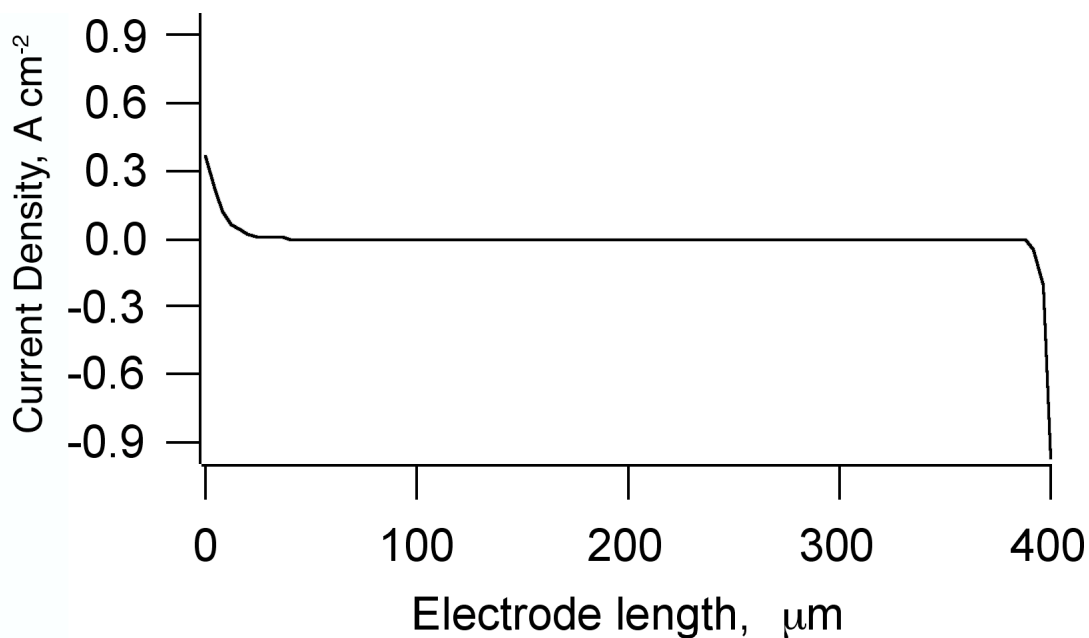


Figure S3. Current distribution on Au with 3V potential difference across the electrode. Cathodic current is positive. Smaller spatial coordinate values correspond to more negative potentials.

densities reported in the literature. In addition, only the geometric area of the electrode is considered in the model. It is typical for electroless gold deposition to yield granular surfaces with a fractal dimension,  $d$ , between 2 and 3.<sup>5,6</sup> Thus, the actual current density required to nucleate and grow gas bubbles in the channel may vary significantly from the calculated value.

## References

1. A. J. Bard and L. R. Faulkner, *Electrochemical Methods: Fundamentals and Applications*, 2nd edn., John Wiley New York, 2001.
2. B. E. Conway, *Progr. Surf. Sci.*, 1995, **49**, 331-452.
3. J. J. MacDonald and B. E. Conway, *Proc. Roy. Soc. Lond. Math. Phys. Sci.*, 1962, **269**, 419-440.
4. T. Ohmori and M. Enyo, *Electrochim. Acta*, 1992, **37**, 2021-2028.
5. T. L. Williamson, X. Y. Guo, A. Zukoski, A. Sood, D. J. Diaz and P. W. Bohn, *J. Phys. Chem. B*, 2005, **109**, 20186-20191.
6. S. Hrapovic, Y. L. Liu, G. Enright, F. Bensebaa and J. H. T. Luong, *Langmuir*, 2003, **19**, 3958-3965.